

A Backstepping Nonlinear Control Approach to Switched Reluctance Motors

Muthana T. Alrifai

Joe H. Chow

David A. Torrey

Department of Electric Power Engineering
Rensselaer Polytechnic Institute
Troy, NY 12180-3590

Abstract

This paper presents the application of backstepping feedback design technique to the speed control of a switched reluctance motor (SRM). Using backstepping method, both feedback laws and Lyapunov based designs are applied in the controller design. The mathematical model for the SRM takes magnetic saturation into account. The controller takes phase currents, rotor position, rotor speed, and reference speed as inputs, and calculates the voltage required to maintain the motor speed close to the reference speed. The turn-on and conduction angles are continuously controlled to improve the system performance. An experimentally verified Saber model is used for simulation. A conventional PI controller is used for comparison. Simulation results confirm reduction in torque ripples, improved transient and steady state performance, and robustness of the controller.

1 Introduction

The SRM is a doubly salient, brushless motor with no winding or magnets on its rotor. Currents in stator phases are controlled based on the rotor position as dictated by an electronic commutator. Unlike DC motors, SRMs are almost maintenance free and less expensive; the absence of mechanical brushes makes them easier to maintain, and having no rotor winding or magnets reduces their costs. Moreover SRMs can produce high torques at low speeds [1]. These characteristics combined with the advanced power electronics, and the availability of high-speed processors make them attractive for many applications such as factory automation.

In contrast, control of the SRM is a nonlinear multivariable problem. The behavior of a SRM and its drive are so nonlinear that modern control methods can hardly be applied in the known manner for integrated manufacturing [2]. The work reported here investigates the development of an appropriate nonlinear control technique which can achieve high dynamical performance as required for variable speed regulation or position tracking. Many of the speed/position controllers reported in the literature are open loop with current and angle control. These controllers do not achieve high dynamic performance which rivals that of a DC drive. Dynamic performance can be improved by feedback control. Closed loop control strategies for SRM are proposed in [3] - [8].

One of the nonlinear control methods that has been applied to feedback control of SRM is feedback linearization. The main idea behind feedback linearization control [9] is to transform the nonlinear system dynamics into a linear form so that classical linear control techniques can be applied to

design the controller. In [10] feedback linearization was applied to SRM, for trajectory tracking in robotics applications. A state feedback control algorithm was designed, on the basis of nonlinear control techniques, which compensates for nonlinearities and decouples the effect of stator phase current in torque production. Another algorithm based on an input/output feedback linearizing control for speed control of the SRM was proposed in [11]. In both [10] and [11], out of the three input variables to the SRM, phase voltage, turn-on angle, and turn-off angle, the phase voltage is used as the only control variable, where the other two are kept fixed.

In [12], the use of a nonlinear adaptive feedback linearizing control to a three-phase SRM was reported. The nonlinear adaptive control structure not only compensates for the nonlinearities between inputs and outputs, it allows the use of linear controllers for motion tracking. However, magnetic saturation was neglected in this work. It is important to emphasize that the SRM operates with significant saturation for high-performance operation of the SRM drive.

A new tool for nonlinear systems feedback design has been introduced in [16]. Backstepping is a recursive design methodology where both feedback control laws and Lyapunov based designs are applied. Unlike feedback linearization which requires precise models, backstepping designs offer a choice of design tools for accommodation of uncertain nonlinearities and can avoid unnecessary cancellations.

In this paper we apply the backstepping technique to design a speed controller for the SRM. The controller takes the phase currents, the rotor position, the rotor speed (actual speed), and the reference speed as inputs. The output is a voltage that is applied to a selected phase by an electronic commutator via a chopper and a power inverter. The turn-on angle and the conduction angle are continuously controlled to maintain the desired reference speed and to optimize the performance.

2 SRM Model

A reliable mathematical model is essential for properly evaluating the SRM performance and effectiveness of different control schemes. Both spatial and magnetic nonlinearities are inherent characteristics of the SRM. The model suggested by [13] which takes magnetic saturation into account is adopted in this work. A 20 kW, 3 phase SRM, which is documented in [13], is used for simulation. It has six stator poles and four rotor poles, as shown in Fig. 1. The choice of high power rating motor reflects the reliability of the proposed speed controller. The motor parameters are provided in the Appendix.

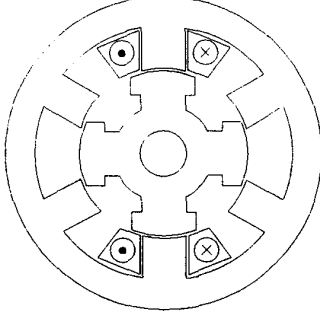


Figure 1: A 3 Phase, 6/4 SRM. Only one phase winding is shown.

In order to express the dynamics of an m phase SRM, we apply Newton's law to the rotor and Kirchoff's law to the stator, to yield the state-space model

$$\frac{d\theta}{dt} = \omega \quad (1)$$

$$\frac{d\omega}{dt} = \frac{1}{J} \{T_e - T_L - D\omega\} \quad (2)$$

$$\begin{aligned} \frac{di_j}{dt} = & - \left(\frac{\partial \lambda_j}{\partial i_j} \right)^{-1} \left\{ Ri_j + \left(\frac{\partial \lambda_j}{\partial \theta} \right) \omega \right\} \\ & + \left(\frac{\partial \lambda_j}{\partial i_j} \right)^{-1} u_j, \quad j = 1, 2, \dots, m \end{aligned} \quad (3)$$

where θ is the rotor position, ω is the rotor speed, T_e is the electromagnetic torque, T_L is the load torque, J is the rotor inertia, D is the damping factor, i_j is the current flowing in the j -th phase, λ_j is the flux-linkage of the j -th phase, R is the ohmic phase resistance, and u_j is the voltage applied to the stator terminals of the j -th phase.

The flux-linkage λ_j is a nonlinear function of the phase current i_j because of magnetic saturation, and a nonlinear function of rotor position due to the periodicity of alignment between stator and rotor poles. The flux linkage is defined [13] as

$$\begin{aligned} \lambda(i_j, \theta) = & a_{1j}(\theta)[1 - e^{a_{2j}(\theta)i_j}] + a_{3j}(\theta) \\ & i_j \geq 0, \quad j = 1, 2, \dots, m \end{aligned} \quad (4)$$

The spatially periodic structure of the machine allows one to express the coefficients a_{1-3} as a truncated Fourier cosine series [13]

$$a_x = \sum_{r=1}^n A_{xr} \cos(\delta\theta r), \quad x = 1, 2, \dots \quad (5)$$

where δ is the number of electrical cycles in each mechanical revolution. The Fourier coefficients are easily determined [13] using the Marquardt gradient expansion algorithm [14].

The torque for phase j , T_{ej} , produced by a SRM with independent phases during both saturated and unsaturated magnetic operation, can be determined according to coenergy analysis [15] as

$$T_{ej} = \frac{\partial}{\partial \theta} \int_0^{i_j} \lambda(i', \theta) di' \quad (6)$$

The sum $T_e = \sum_j T_{ej}$ of the individual phase torques gives the total torque. Substitution of Eqn. 4 into Eqn. 6 gives the total torque produced by phase j

$$\begin{aligned} T_{ej} = & \sum_{j=1}^m \left\{ \left[i_j + \frac{1}{a_{2j}} (1 - e^{a_{2j}i_j}) \right] \frac{da_{1j}}{d\theta} \right. \\ & - \left[\frac{a_{1j}}{a_{2j}^2} (1 - e^{a_{2j}i_j}) + \frac{a_{1j}i_j}{a_{2j}} e^{a_{2j}i_j} \right] \frac{da_{2j}}{d\theta} \\ & \left. + \frac{1}{2} i_j^2 \frac{da_{3j}}{d\theta} \right\} \end{aligned} \quad (7)$$

where

$$\frac{da_{xj}}{d\theta} = \sum_{r=1}^n -r\delta A_{xr} \sin(r\delta(\theta + (j-1)120^\circ)) \quad (8)$$

and all of the coefficients $a_{1-3}(\theta)$ and their derivatives include the appropriate phase shifting of rotor position [13]. In the linear region Eqn. 7 can be simplified to

$$T_{ej} = \sum_{j=1}^m k_j(\theta) i_j^2 \quad (9)$$

where

$$k_j(\theta) = \frac{1}{2} \left[-a_{2j} \frac{da_{1j}}{d\theta} - a_{1j} \frac{da_{2j}}{d\theta} + \frac{da_{3j}}{d\theta} \right] \quad (10)$$

The output of the system can be taken as the rotor position θ or the speed ω , whereas u_j acts as the control input. An electronic commutator decides which phase to be excited at any given instant of time based on rotor position information.

At low speed, pulse-width modulation of the applied voltage or current regulation about a predetermined reference current has been used to control the SRM. This type of control produces a constant-torque characteristic. To obtain speed control, a speed feedback loop is necessary. The control parameters available are the terminal voltage, the turn-on angle, and the turn-off angle (or excitation angles). Although it is possible to control the SRM by varying the terminal voltage, control of the excitation angles optimize overall system performance and increase the speed range.

3 Control Strategies

The nonlinear block backstepping algorithm is discussed first in Section 3.1. Its application to the SRM is then detailed in Section 3.2. Implementation is in Section 3.3, followed by excitation angle control in Section 3.4.

3.1 Nonlinear Block Backstepping

Consider the system

$$\dot{x} = f(x) + g(x)u, \quad f(0) = 0, \quad V(x) > 0 \quad (11)$$

where $x \in R^n$ is the state, and $u \in R$ is the control input. Let $u_{des} = \alpha(x)$, $\alpha(0) = 0$, be a desired stabilizing feedback control law, which, if applied to system 11, guarantees global boundedness and regulation of $x(t)$ to the

equilibrium point $x = 0$ as $t \rightarrow \infty$, for all $x(0)$ and $V(x)$ is a control Lyapunov function, where

$$\frac{\partial V(x)}{\partial x} [f(x) + g(x)\alpha(x)] < 0 \quad (12)$$

Consider the following cascade system

$$\begin{aligned} \dot{x} &= f(x) + g(x)y, \quad f(0) = 0 & (13a) \\ \dot{\zeta} &= m(x, \zeta) + \beta(x, \zeta)u, \quad y = h(\zeta), \quad h(0) = 0 & (13b) \end{aligned}$$

where for system 13a, a desired feedback $\alpha(x)$ and a control Lyapunov function $V(x)$ are known. Then using the nonlinear block backstepping theory in [16], the error between the actual and the desired input for system 13a can be defined as $z = y - \alpha$, and an overall control Lyapunov function $V(x, \zeta)$ for both systems 13a and 13b can be defined by augmenting a quadratic term in the error variable z with $V(x)$:

$$V(x, \zeta) = V(x) + \frac{1}{2}z^2 \quad (14)$$

Taking the derivative of both sides, we obtain

$$\dot{V}(x, \zeta) = \dot{V}(x) + z\dot{z} \quad (15)$$

from which solving for $u(x, \zeta)$, which renders $\dot{V}(x, \zeta)$ negative definite, yields a feedback control law for the full system 13. One particular choice is [16]

$$u = \left(\frac{\partial h(\zeta)}{\partial \zeta} \beta(x, \zeta) \right)^{-1} \left\{ -c(y - \alpha) - \frac{\partial h(\zeta)}{\partial \zeta} m(x, \zeta) + \frac{\partial \alpha(x)}{\partial x} \dot{x} - \frac{\partial V(x)}{\partial x} g(x) \right\}, \quad c > 0 \quad (16)$$

3.2 Application to SRM

Rewriting Eqn. 2 and Eqn. 3 of the SRM model to match Eqn. 13 yield,

$$\begin{aligned} \frac{d\omega}{dt} &= \frac{1}{J} \{-T_L - D\omega\} + \frac{1}{J} k(\theta) i^2 \\ &= f(\omega, \theta) + g(\omega, \theta) y \end{aligned} \quad (17a)$$

$$\begin{aligned} \frac{di}{dt} &= - \left(\frac{\partial \lambda}{\partial i} \right)^{-1} \left\{ Ri + \left(\frac{\partial \lambda}{\partial \theta} \right) \omega \right\} + \left(\frac{\partial \lambda}{\partial i} \right)^{-1} u \\ &= m(\omega, i, \theta) + \beta(\omega, i, \theta) u \end{aligned} \quad (17b)$$

where $y = i^2$ is a virtual input for Eqn. 17a, u is the control input for Eqn. 17b, ω is the speed, and i is the current. The rotor position θ is taken as a time varying parameter in the control design. The control

$$y_{des} = \alpha = \frac{1}{k(\theta)} \{T_L + D\omega - p(\omega - \omega_{ref})\}, \quad p > 0$$

if applied to system 17a cancels the terms in it and replaces them by

$$\dot{\omega} = \frac{-p}{J} (\omega - \omega_{ref})$$

so that the resulting feedback system is linear in ω .

Consider

$$V(\omega) = \frac{q}{2} (\omega - \omega_{ref})^2, \quad q > 0$$

as a Lyapunov function for system 17a, where $V(\omega) > 0$ and $\dot{V}(\omega) < 0$. Let z be the deviation of y from α (y_{des}), then

$$z = y - \alpha \quad (18)$$

According to [16], a Lyapunov function $V(\omega, i, \theta)$ for the overall system, system 17, can be constructed by augmenting $V(\omega)$ with a quadratic term in the error variable z :

$$V(\omega, i, \theta) = V(\omega) + \frac{1}{2}z^2 \quad (19)$$

Taking the derivative of both sides,

$$\begin{aligned} \dot{V}(\omega, i, \theta, u) &= \dot{V} + z\dot{z} \\ &= \frac{\partial V}{\partial \omega} (f + gy) + z(\dot{y} - \dot{\alpha}) \\ &= \frac{\partial V}{\partial \omega} (f + g\alpha + gz) + z(\dot{y} - \dot{\alpha}) \\ &= \frac{\partial V}{\partial \omega} (f + g\alpha) + z \left(\frac{\partial h}{\partial i} m + \frac{\partial h}{\partial i} \beta u - \frac{\partial \alpha}{\partial \omega} \dot{\omega} + \frac{\partial V}{\partial \omega} g \right) \end{aligned} \quad (20)$$

Based on Eqn. 16, u that renders $\dot{V}(\omega, i, \theta, u) < 0$ is

$$\begin{aligned} u &= \left(\frac{\partial h}{\partial i} \beta \right)^{-1} \left\{ -c(y - \alpha) - \frac{\partial h}{\partial i} m + \frac{\partial \alpha}{\partial \omega} \dot{\omega} - \frac{\partial V}{\partial \omega} g \right\} \\ &= u_1 + u_2 + u_3 + u_4, \quad c > 0 \end{aligned} \quad (21)$$

where

$$\begin{aligned} u_1 &= \frac{-c}{2i} \left(\frac{\partial \lambda}{\partial i} \right) \left[i^2 - \left(\frac{T_L + D\omega - p(\omega - \omega_{ref})}{k(\theta)} \right) \right] \\ u_2 &= Ri + \left(\frac{\partial \lambda}{\partial \theta} \right) \omega \\ u_3 &= \frac{D - p}{2iJk(\theta)} \left(\frac{\partial \lambda}{\partial i} \right) \{-T_L - D\omega + k(\theta)i^2\} \\ u_4 &= \frac{-qk(\theta)}{2iJ} \left(\frac{\partial \lambda}{\partial i} \right) (\omega - \omega_{ref}) \end{aligned}$$

where $\frac{\partial \lambda}{\partial i}$ and $\frac{\partial \lambda}{\partial \theta}$ are the partial derivatives of Eqn. 4 with respect to i and θ respectively. The controller parameters p, q, c and c are tuned according to their effect on the feedback control law.

3.3 Implementation

Figure 2 shows the backstepping controller based drive system for speed control of SRM. It consists of an inner current loop and an outer speed loop. The power inverter used for simulation is a two switch per phase bridge inverter. The backstepping controller takes the phase currents, rotor position, rotor speed, and reference speed as inputs and calculates the control voltage u required to maintain the motor speed ω close to the reference speed ω_{ref} . The output u of the backstepping controller is applied to a chopper which converts the fixed DC source to the required variable output voltage v . Only one chopper is needed for the three phase SRM. This variable voltage is then applied to the power inverter and ultimately to the selected phase dictated by the electronic commutator. The electronic commutator takes rotor position θ , turn-on angle θ_{on} , and turn-off angle θ_{off} as inputs and decides which phase to be excited at a given instant of time.

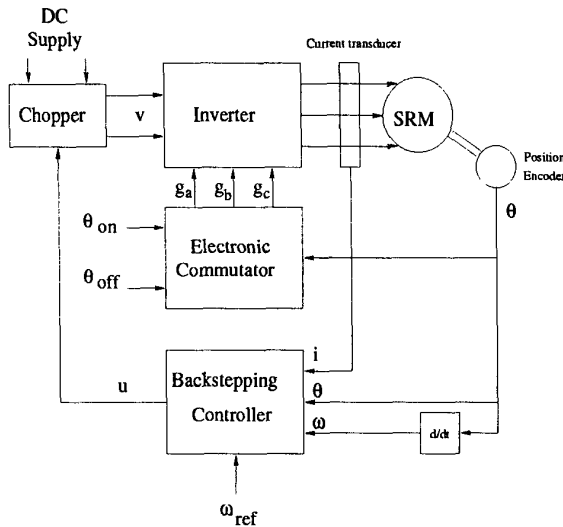


Figure 2: Backstepping controller based drive system for speed control of SRM.

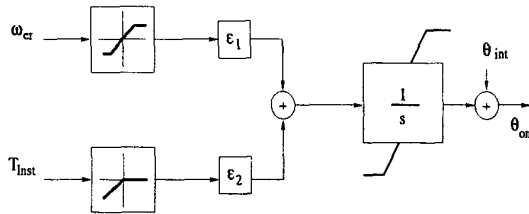


Figure 3: Adaptive loop to control turn-on and conduction angles.

3.4 Excitation Angle Control

When turn-on and conduction angles are kept fixed, the performance of the backstepping controller is acceptable only for a limited range of speed and load torque. This is due to the operational characteristics of the SRM. To improve and optimize the performance, control of excitation angles is needed.

In Fig. 2, the turn-on and the conduction angles are provided to the electronic commutator and kept fixed, whereas in this section an adaptive setpoint control is proposed. The speed error, $\omega_{er} = \omega - \omega_{ref}$, and the instantaneous torque T_{Inst} , are fed back to a nonwindup integral controller, then to the electronic commutator, as shown in Fig. 3. The instantaneous torque T_{Inst} is calculated based on Eqn. 7 which is valid for both saturated and unsaturated magnetic operations. The output of the integrator is algebraically added to an initial turn-on angle θ_{int} . Not only is advancing or retarding the turn-on angle achieved, the conduction is increased or decreased as well because the turn-off angle is kept constant. Based on the instantaneous torque we avoid advancing the turn-on angle to the region where negative torque is produced, as a result the instantaneous torque signal is active only when negative torque is produced. This technique improves the performance to the extent that high torque ripples are avoided. Moreover, a wider speed range can be achieved. The constants ε_1 and ε_2 are the integral gains scaled according to the effects of the input signals.

4 Simulation Results

The backstepping controller based drive for speed control of a SRM has been simulated using the Saber simulator [18]. The experimentally verified SRM Saber model described in [19] has been used. The motor parameters are provided in the Appendix.

For a comparison of controller performance, a PI speed controller is designed for the SRM and simulated. The output of the controller is applied to a chopper that controls the duty cycle and as a result, the applied voltage to the phase winding.

4.1 Performance of PI Controller

The PI control law

$$u = k_P \omega_{er} + k_I \int \omega_{er} dt$$

is used for simulation studies. The gains k_P and k_I are tuned manually for low speed and low load torque operations. Figure 4 shows the speed response of the motor. It can be seen that the controller parameters are well tuned for speed of 100 rad/s and load torque of 25 N.m, but for step change in the speed from 100 to 200 rad/s, the response has higher overshoot and needs more time to settle. Such performance does not meet the required specifications for high performance drive applications. For this SRM, it is not possible to obtain a single fixed PI controller to achieve good performance over a wide speed and load range. This demonstrates the main draw back of a PI controller.

4.2 Performance of Backstepping Controller

4.2.1 Fixed Excitation Angles: The turn-on and the turn-off angles are kept constant throughout the simulation at 45° and 74° , respectively (where 0° and 90° correspond to aligned and unaligned positions). Figure 5 shows the speed response of the motor when it is allowed to accelerate from rest to a reference speed of 100 rad/s, then to 200 rad/s with a load torque of 25 N.m. It can be seen that the speed response has improved compared to Fig 4, especially the rise time and the settling time. Figure 6 shows the electromagnetic torque associated with both reference speeds.

Figure 7 shows the speed response for step changes in the reference speed. The reference speed is increased from rest to 100 rad/s as before, then from 100 to 200 rad/s, followed by drop to 100 rad/s, with constant load of 100 N.m. It can be seen that the motor speed could not track the reference speed with fixed excitation angles. It should be noted that this is not due to the backstepping controller, but due to the motor operational characteristic and limits of the electronic commutator. Figure 8 shows the voltage waveform for one phase only, corresponding to Fig. 7. It can be noticed that the controller is commanding almost 100% duty cycle to track the reference speed. A solution to improve the speed response is to advance the turn-on angle. Moreover, it can be seen that the magnitude of the phase voltage is not fixed at the DC source (-230 or 230 V), but it has variable magnitude to compensate for the nonlinearities.

4.2.2 Performance with Excitation Angle Control: To improve the performance at higher speeds, the turn-on angle should be advanced to allow for more current to build up to counter the back EMF and to obtain the desired speed. For this purpose, the setpoint adaptive

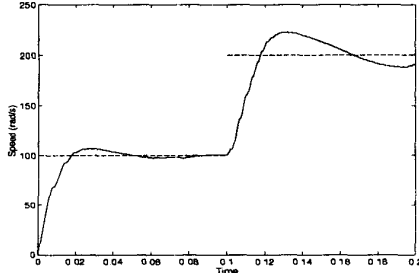


Figure 4: Speed response of SRM drive under PI control for step changes in reference speed from 0 to 100 rad/s for time $t = 0.0 - 0.1$ s and from 100 to 200 rad/s for time $t = 0.1 - 0.2$ s with load torque of 25 N.m.

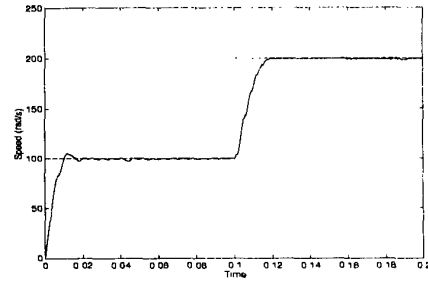


Figure 5: Speed response of SRM drive under backstepping control for step changes in reference speed from 0 to 100 rad/s for time $t = 0.0 - 0.1$ s and from 100 to 200 rad/s for time $t = 0.1 - 0.2$ s with load torque of 25 N.m.

feedback loop shown in Fig. 3 has been implemented. To show that a wider speed range is maintained with excitation angle control, Fig. 9 shows the speed response when the motor starts from rest to 200 rad/s with a load torque of 100 N.m, followed by a change in the reference speed to 300 rad/s, then a drop to 100 rad/s. It can be noticed that the motor speed is almost tracking the reference speed. Moreover, when the motor is allowed to accelerate from rest to a reference speed of 200 rad/s, with a load of 100 N.m, the speed response has no overshoot or oscillations. The turn-on angle is shown in Fig. 10. It can be seen how the turn-on angle is advanced and retarded based on the desired speed and load. The torque response of the motor under fixed and controlled excitation angles is shown in Fig. 12, the motor is allowed to accelerate from rest to 200 rad/s with a load torque of 100 N.m. It can be noticed that the performance with excitation angle control has improved since torque ripples are reduced, and as a result reduction in the acoustic noise is expected.

4.2.3 Effect of Load Torque: In Eqn. 21, the load torque information is needed, specifically in u_1 and u_3 . To show the robustness of the controller during load disturbances, the load torque was changed from 100 to 50 N.m and subsequently increased to 75 N.m for a reference speed of 200 rad/s. Moreover, no information about the load torque is provided to the controller. That is, the term T_L is set to zero in u_1 and u_3 . Figure 11 shows the corresponding speed responses. It can be seen that when the load torque is decreased the speed increases but the controller is able to hold the motor speed close to the reference speed. However, when the load torque is increased there is a slight dip in the speed, but again the controller is able to bring the motor speed back close to the reference value.

5 Conclusions

The design of a backstepping controller for speed tracking application for a SRM has been presented in this paper. Control of excitation angles has been taken into consideration. An experimentally verified SRM Saber model which takes magnetic saturation into account was used for simulation studies. The simulation results show that the backstepping controller is superior to the conventional PI controller in reducing overshoot, settling time, and steady state error, thus providing faster dynamic response. Moreover, the controller parameters once selected provide good performance for the entire operating range. It has been shown by simulation how the control of excitation angles widens the speed range and reduces the torque ripples. The simulation re-

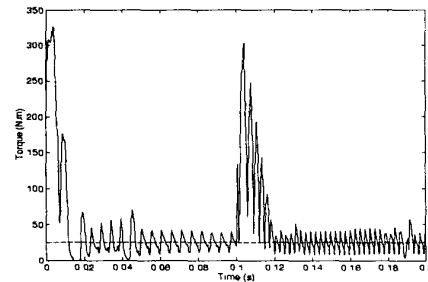


Figure 6: Motor torque response when motor accelerates from rest to 100 rad/s and then to 200 rad/s, with load torque of 25 N.m.

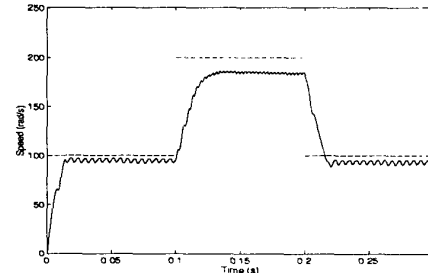


Figure 7: Speed response of SRM drive under backstepping control for step changes in reference speed from 0 to 100 rad/s for time $t = 0.0 - 0.1$ s, from 100 to 200 rad/s for time $t = 0.1 - 0.2$ s, and from 200 to 100 rad/s for time $t = 0.2 - 0.3$ s with load torque of 100 N.m.

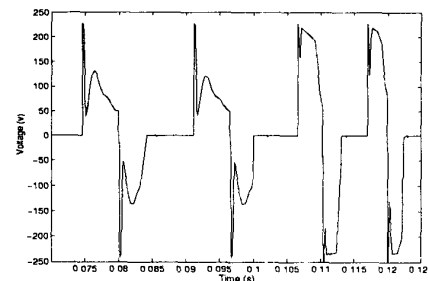


Figure 8: Phase voltage waveform when reference speed is increased from 100 to 200 rad/s with load torque of 100 N.m.

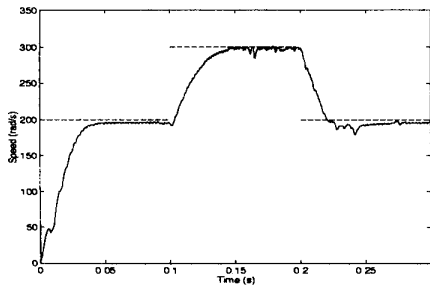


Figure 9: Speed response of SRM drive under backstepping control and excitation angle control for step changes in reference speed from 0 to 200 rad/s for time $t = 0.0 - 0.1s$, from 200 to 300 rad/s for time $t = 0.1 - 0.2s$, and from 300 to 100 rad/s for time $t = 0.2 - 0.3s$ with load torque of 100 N.m.

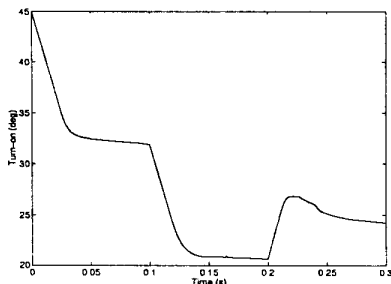


Figure 10: The change in turn-on angle for step changes in reference speed from 0 to 200 rad/s for time $t = 0.0 - 0.1s$, from 200 to 300 rad/s for time $t = 0.1 - 0.2s$, and from 300 to 100 rad/s for time $t = 0.2 - 0.3s$ with load torque of 100 N.m.

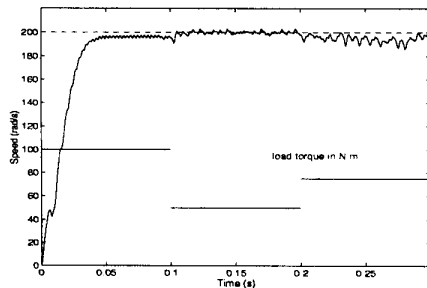


Figure 11: Speed response of SRM drive under backstepping control and excitation angle control for a speed reference of 200 rad/s and step changes in load torque from 100 to 50 N.m for time $t = 0.1 - 0.2s$, and from 50 to 75 N.m for time $t = 0.2 - 0.3s$.

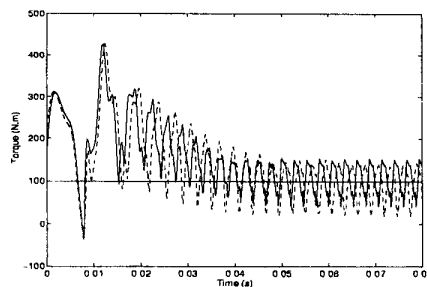


Figure 12: Motor torque response when motor accelerates from rest to 200 rad/s with load torque of 100 N.m, the dashed line is for fixed excitation angles and the solid line is for excitation angles control.

sults also demonstrate the robustness of the backstepping controller.

APPENDIX

Motor parameters:

Output power = 20 kW, Rated speed = 492 rad/s, Number of phases

$m = 3$, Number stator poles = 6, Number rotor poles = 4

Aligned phase inductance $L_a = 19.0$ mH

Unaligned phase inductance $L_u = 0.67$ mH

Inertia $J = 0.02$ N.ms², Damping factor $D = 0.3301$ m N.ms

DC voltage supply = 230 V

Parameters of PI controller:

$k_p = 0.5$, $k_i = 150$

Parameters of backstepping controller:

$p = 1$, $q = 5000000$, $c = 1$

Parameters of adaptive loop:

$\epsilon_1 = 0.4$, $\epsilon_2 = 0.05$

References

- [1] L.-C. R. Zai, D. G. Manzer, and C.-Y. D. Wong, "High-Speed Control of Variable Reluctance Motors with Reduced Torque Ripple," *IEEE*, pp. 107-113, 1992.
- [2] T. J. E. Miller, *Brushless Permanent-magnet and Reluctance Motor Drives*. Clarendon Press, 1989.
- [3] B. K. Bose, T. J. E. Miller, P. M. Szczyzny, and W. H. Bicknell, "Microcomputer Control of Switched Reluctance Motor," *Proc. IEEE/IAS Annual Meeting*, Toronto, pp. 542-547, 1985.
- [4] J. Ish-Shalom and D. G. Manzer, "Commutation and Control of Step Motors," *Proc. 14th Symp. Incremental Motion, Control Systems and Devices*, pp. 283-292, 1985.
- [5] M. Ilic-Spong, T. J. E. Miller, S. R. MacMinn, and J. S. Thorp, "Instantaneous Torque control of Electric Motor Drives," *Proc. IEEE Power Electron. Specialists Conf.*, Toulouse, France, pp. 42-48, 1985; also in *IEEE Trans. Power Electron.*, 1987.
- [6] J. V. Byrne, M. F. McMullin, and J. B. O'Dwyer, "A High Performance Variable Reluctance Drive," *Proc. Motorcon Conf.*, Chicago, IL, pp. 147-160, 1985.
- [7] M. G. Egan, J. M. D. Murphy, P. F. Kenneally, J. V. Lawton, and M. F. McMullin, "A High Performance Variable Reluctance Drive: Achieving Servomotor control," *Proc. Motorcon Conf.*, Chicago, IL, pp. 161-168, 1985.
- [8] J. V. Byrne and F. Devitt, "Design and Performance of a Saturable Variable Reluctance Servo Motor," *Proc. Motorcon Conf.*, Chicago, IL, pp. 139-146, 1985.
- [9] J. E. Slotine and W. Li, *Applied Nonlinear Control*. Prentice-Hall Inc, 1991.
- [10] M. Ilic-Spong, R. Marina, S. M. Persada, and D. G. Taylor, "Feedback Linearizing Control of Switched Reluctance Motors," *IEEE Trans. on Automatic Control*, Vol. AC-32, No. 5, pp. 371-379, 1987.
- [11] S. K. Panda and P. K. Dash, "Application of Nonlinear Control to Switched Reluctance Motors: a Feedback Linearization Approach," *IEE Proc.*, Vol. 143, No. 5, pp. 371-379, 1996.
- [12] L. B. Amor, A. Dessiantl, O. Akhrif, and G. Oliver, "Adaptive Feedback Linearization for Position Control of a Switched Reluctance Motor: Analysis and Simulation," *Int. J. Adapt. Control Signal Process.*, 7, pp. 117-136, 1993.
- [13] D. A. Torrey, and J. H. Lang, "Modeling a Nonlinear Variable Reluctance Motor Drive," *IEE Proc.*, Vol. 137, pt. B, pp. 314-326, 1990.
- [14] P. R. Bevington, *Data Reduction and Error Analysis for the Physical Sciences*. John Wiley & Sons, 1969.
- [15] P. Materu and R. Krishnan, "Estimation of Switched Reluctance Motor Losses," *IEEE/IAS Annual Meeting Conference Record*, pp. 79-89, 1988.
- [16] M. Krstic, I. Kanellakopoulos, and P. Kokotovic, *Nonlinear and Adaptive Control Design*, Wiley-Interscience, 1995.
- [17] T. J. E. Miller, P. G. Bower, R. Becerra, and M. Ehsani, "Four-Quadrant Brushless Reluctance Motor Drive," *IEE Conf. on Power Electronics and Variables Speed Drives*, London, 1988.
- [18] Analogy, Inc., *An Introduction to the Saber Simulator*, 1992.
- [19] D. A. Torrey, "An Experimentally Verified Variable-Reluctance Machine Model Implemented in the Saber Circuit Simulator," *Electric Machines and Power Systems*, Vol. 24, pp. 199-210, 1996.